Strain-Induced Transformation of Very Strong Metal

Mohamed Youssef Sherif
St Edmund's College

University of Cambridge
Department of Materials Science and Metallurgy
Pembroke Street, Cambridge CB2 3QZ

A dissertation submitted for the degree of Master of Philosophy in Materials Modelling at the University of Cambridge
August 2003

Index

Preface

This dissertation is submitted for the degree of Master of Philosophy in Materials Modelling at the University of Cambridge. The research described herein was conducted under the supervision of Professor H. K. D. H. Bhadeshia and Dr C. Garcia Mateo in the Department of Materials Science and Metallurgy, University of Cambridge, between May 2003 and August 2003.

Except where acknowledgements and references are made to previous work, this work is, to the best of my knowledge, original. Neither this, nor any substantially similar dissertation has been or is being submitted for any other degree, diploma or other qualification at any other university. This dissertation contains less than 15,000 words.

Part of this work has been submitted to appear in the following publication:

M. Sherif, C. Garcia Mateo, T. Sourmail and H. K. D. H. Bhadeshia, *Stability of Retained Austenite in TRIP–Assisted Steels*, Materials Science and Technology, *submitted* (2003).

Mohamed Sherif

August 2003

Acknowledgements

I am very grateful to my supervisors Prof. H. K. D. H. Bhadeshia and Dr C. Garcia Mateo for their encouragement during this work. I would like to thank Prof. M. M. I. Hammouda, Prof. N. Fatahalla, Prof. M. Elkady and Mrs Manal Shaheen for their continuous encouragement and support. I would like also to thank all those who have contributed to the Materials Modelling course and all the members of the Phase Transformations group.

I am indebted to Cambridge Overseas Trust for funding this project.

Finally, I would like to thank my parents and my friends for their love and support.

Abstract

A theory was proposed as an attempt to represent quantitatively the strain-induced transformation behaviour of austenite (γ) to martensite (α') in low-alloy TRIP (transformation-induced plasticity) aided steels. The theory for the first time allows the estimation of the amount of austenite transformed as a function of plastic strain (ε). Deformation temperature, chemical composition and hydrostatic pressure effects are considered and introduced through the free energy available for transformation $\Delta G^{\gamma\alpha}$. It was possible therefore not only to predict the transformation behaviour of austenite but also its stability. Calculated results based on the proposed models showed good agreement with published experimental data which were used to validate the theory.

At high temperatures and high carbon or manganese concentrations, the retained austenite was, as expected, found to be more resistant to strain. This behaviour is consistent with the literature[1,32,49]. The theory is therefore capable of predicting the mechanical stability of austenite, which is a crucial issue in the context of TRIP-aided alloys of the type developed for the automobile industry.

It was possible to estimate the hydrostatic pressure effect on transformation through altering the free energy available for transformation[46]. It is expected that hydrostatic pressure decreases the transformation rate by opposing the volume expansion due to transformation.

Unlike previously proposed models[32-37], it was possible to propose a general model that is alloy-independent, *i.e.* uses universal values for the single fitting constant.

It was also possible to calculate the M_d temperature (which is the temperature at which transformation is not expected to occur, no matter how much stress or strain is applied) for

any alloy given its chemical composition. The estimation of M_d has not previously been possible. The M_d temperature showed a strong dependence on alloy chemical composition.

Chapter 1

Introduction

1.1 Overview

Conventional high strength dual-phase steels have been used widely in the automobile manufacturing industry to meet the increased demand for safety and weight reduction for both economical and environmental considerations. However, the drawback of using such high strength levels is that high strength alloys generally have less ductility. This is a particular disadvantage in metal-forming operations which demand a significant amount of ductility. Low-alloy TRIP-aided multiphase steels with a microstructure consisting of intercritical ferrite, retained austenite, bainite and sometimes martensite, can be a potential and promising substitute to conventional high strength dual-phase steels giving the observed high ductility of theses alloys due to the TRIP effect[6]. TRIP-aided steels exhibit excellent strength-ductility combinations due to the presence of retained austenite that transforms into martensite during plastic straining results in the delay of the onset of necking[1-5]. Furthermore, low-alloy TRIP steels are economically very competitive hence there is no need for expensive alloying elements as is the case with conventional TRIP-aided steels which usually contain relatively high amounts of nickel and chromium.

The TRIP effect was first discovered by Zackay *et al.*[6]. It is thought to be responsible for the significant increase in the total elongation and consequently ductility of TRIP-aided steel alloys. The enhanced uniform ductility of TRIP steels is ascribed to the process of plastic accommodation in the vicinity of martensite plates[7]. Nevertheless, to achieve such a significant ductility improvement, the uniform elongation during plastic straining needs to be

maximised. Rapid austenite transformation to martensite in the early stages of deformation has been reported to be detrimental to ductility. As such, the most important parameter to control is therefore the stability of the retained austenite.

1.2 Preparation of TRIP Steels

1.2.1 Heat-treatment

Hence the strain-induced transformation of the austenitic phase is responsible for the ductility enhancement of TRIP steels, obtaining a sufficient percentage of retained austenite in the microstructure is the first step to be considered while developing TRIP-aided steels. Two-stage special heat-treatment technique has been used widely to obtain an optimum amount of retained austenite in the alloy[8].

1.2.1.1 Intercritical Annealing

The first stage is intercritical annealing which has traditionally been used to obtain an amount of austenite in the microstructure via heating cold-rolled strips from room temperature to the intercritical annealing temperature region. In the iron-carbon equilibrium phase diagram, the intercritical annealing regime is identified as the region within the Ae_1 - Ae_3 temperature range. These temperatures[8] are often referred to as the "critical temperatures" which can be estimated by using the empirical formula given by Andrews[9]. At temperatures between Ae_1 and Ae_3, the microstructure is typically allotriomorphic ferrite plus austenite. However, at temperatures above Ae_3, the microstructure is fully austenitic as is the case with hot-rolled steels. Applying the necessary heat-treatment processes starting from the hot-rolled condition can be beneficial especially from an economical point of view hence there is no need to re-heat the strips from the room temperature[8]. Fig. 1 shows the isothermal transformation

diagram[10] of the cooling-induced phase transformations in steels representing the intercritical annealing temperature regime identified by the temperatures Ae_1 and Ae_3.

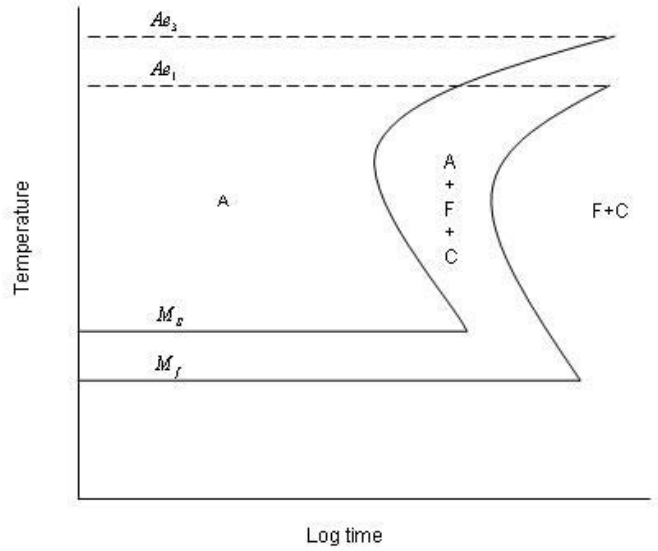

Fig. 1: TTT (time-temperature-transformation) diagram representing phase transformations in steels. Isothermal phase transformations are given as a function of temperature and time. The temperature range between Ae_1 and Ae_3 represents the intercritical annealing range. M_S and M_f are the martensite start and finish temperatures respectively. A, F and C are austenite, ferrite and cementite respectively.

Matsumura *et al.*[11] have investigated the effect of the annealing temperature on the mechanical properties of a TRIP steel of the composition 0.4C-1.5Si-0.8Mn wt%. The holding time during the intercritical annealing process was 5 min. Bainitic transformation was carried out at 400 °C for 5 min. In their work, they reported the increase in the tensile strength of the alloy by raising the annealing temperature from below Ae_1 to 840 °C which was above

Ae_3. The tensile strength enhancement which was more than about 60%, was due to obtaining a final microstructure of 90% bainite when annealing at 840 °C, above Ae_3, compared with ferrite plus pearlite when annealing was carried out at below Ae_1. They reported also that, as the annealing temperature increased to just above Ae_1, there was a significant increase in elongation due to obtaining the austenitic phase in the microstructure. However, there was a drop in the elongation for relatively higher annealing temperatures due to the decrease in the volume fraction of ferrite and the increase of bainite volume fraction with a slight decrease in the retained austenite content. This drop in the elongation may be explained in the light of the dependence between the volume fraction of ferrite and the carbon content in the austenite[12]. This is to conclude that, the nature of the second phase also contributes to the overall ductility improvement. Needless to say, the holding time in the intercritical annealing region is also important. Insufficient holding time results in low tensile strength and elongation levels[11]. It is therefore important to select the optimum intercritical annealing conditions for a certain bainitic transformation process. They suggested that, for the alloy studied, and for the given bainitic transformation, optimum strength-ductility combination was at an annealing temperature just above Ae_1.

1.2.1.2 Bainite Transformation

The second stage involves a controlled cooling rate to the bainitic transformation temperature region through which isothermal holding takes place.

The final microstructure after the two-stage heat-treatment process is typical of intercritical ferrite and austenite resulting from the first stage, the intercritical annealing, and upper bainite resulting from bainitic transformation in the second stage. Bainitic transformation encourages the carbon to partition into the residual austenite. As reported in the literature[1,13], the carbon-enriching process stabilises austenite and makes it more resistant to transformation to martensite. The stabilising effect is essential not only to resist transformation during the final cooling to room temperature[13] but, also, to make it less sensitive to applied chemical and or mechanical driving forces during the plastic deformation of the steel.

Many authors have reported the effect of varying the holding time in the bainite transformation temperature region on the mechanical properties especially on the total elongation, for example as reported by Matsumura *et al.*[1]. It is reported that by varying the holding time during bainitic transformation, the carbon concentration in austenite (C_γ) changes as a carbon re-distribution process takes place. In fact, varying the holding time in the bainite transformation temperature region has a strong connection with the stability of austenite and hence the mechanical properties or in particular the total elongation of the alloy concerned. It is well known that the increase of the austenite carbon content has the effect of decreasing the temperature at which martensite starts to form by cooling[14]. This is to conclude that the austenite becomes more resistant to transformation into martensite.

Fig. 2 shows the degree of austenite stability versus strain[15]. As shown in Fig. 2, by increasing the holding time in the bainite transformation range, the mechanical stability of the retained austenite has significantly increased as more carbon partitioned from the ferritic bainite enriches the intercritical austenite. Nevertheless, at prolonged holding time at the bainitic

transformation range, the total elongation decreases as the volume fraction of retained austenite decreases[11].

The mechanical stability of austenite due to carbon enrichment supports the approach in the present work, to consider the austenitic chemical composition in any theory. The composition has a direct effect on the free energies of the phases and consequently on the strain-induced transformation behaviour as a whole.

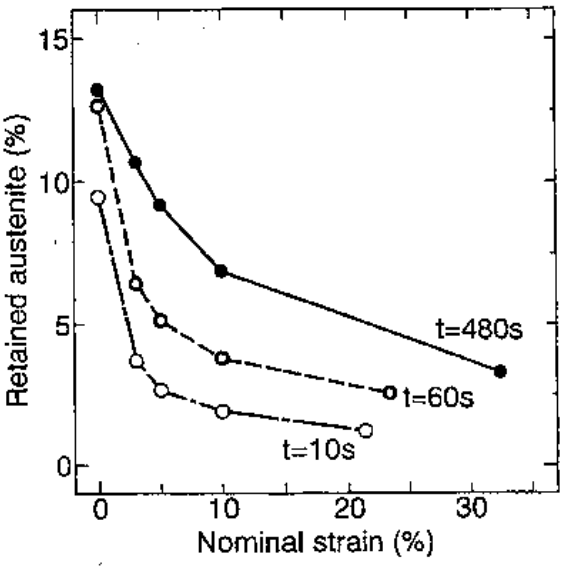

Fig. 2: A plot of retained austenite percentage versus strain. The graph represents the strain-induced transformation behaviour of austenite as the holding time during bainitic transformation varies[15].

Retained austenite morphology has an effect on its mechanical stability and consequently on the total elongation of the alloy. The morphology can be controlled by adjusting the heat-treatment parameters so as to produce the desired morphology of the phases in the microstructure. Sugimoto *et al.*[16] have investigated the morphology effects of both austenite and the second phase (a mixture of bainite and retained austenite particles) morphologies on

the mechanical properties of a TRIP-aided dual-phase steel of the composition 0.17C-1.41Si-2.00Mn wt%. Three different heat-treatments procedures were followed to obtain different morphologies of the retained austenite. Retained austenite grains were in the form of:

1) Isolated islands in the intercritical ferrite matrix.
2) Thin films distributed along bainitic laths.
3) Isolated islands of fine and acicular austenite in the ferrite matrix.

The best elongation behaviour is said to be when retained austenite is in the form of thin films embedded between bainite sub-units rather than as blocky grains.

Furthermore, the retained austenite grain size may have an effect on the transformation behaviour during plastic deformation. At grain sizes below about 10 μm, the interfacial energy due to the forming of a martensitic plate within an austenitic grain increases exponentially[12]. The rate of increase of the interfacial energy is expected obviously to vary with different aspect ratios (the aspect ratio is the ratio of the plate width to its length) of the martensitic plates, however, in general, there is a significant increase in the necessary driving force for transformation as the grain size decreases below about 10 μm resulting in more austenite stability.

It is also important to note that at austenite grain sizes of about 0.01 μm or smaller, transformation into martensite does not occur due to the impractical levels of the driving force necessary to accomplish the transformation[12]. Relatively large retained austenite grains were also reported to transform into martensite easily with a significant drop of the total elongation[3]. However, by reducing the temperature at which the bainitic transformation is conducted, the blocky austenite grains can be eliminated[8].

This is to confirm that adjusting the heat-treatment parameters is of obvious effect on the microstructure, the transformation behaviour of the retained austenite and consequently on the overall mechanical properties of TRIP-aided steels.

1.2.2 Microstructure

A typical base chemical composition of low-alloy TRIP-aided steels is Fe-0.15C-1.5Si-1.5Mn wt%. Although there is an apparent simplicity in the chemical composition of these alloys, applying different heat-treatment procedures as presented in section 1.2.1 gives a wide variety of microstructures and mechanical properties. Fig. 3 shows a wide range of mechanical properties that can be obtained in low-alloy TRIP-aided steels[8].

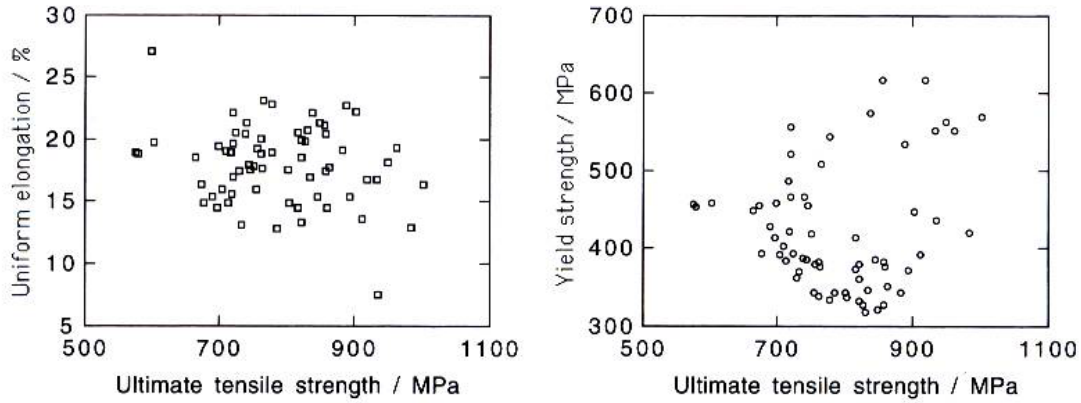

Fig. 3: A plot shows the wide range of mechanical properties achievable in low-alloy TRIP-aided steels of the microstructure containing allotriomorphic ferrite, bainite, martensite and retained austenite[8]. Results presented are of alloys produced with a range of processing conditions with the base composition range of 0.15-0.25C, 0.9-2.0Si and 1.4-1.8Mn wt%.

1.2.3 Silicon Content

It is a common practice in low-alloy TRIP-aided steels to add a larger than usual amount of silicon. That is to ensure that cementite precipitation is not likely to occur in the microstructure during the growth of upper bainite. The absence of cementite ensures high ductility levels by forcing the carbon to enrich the austenite rather to form cementite plates. It has been concluded that austenite retention in these low-alloy steels is almost impossible with silicon concentrations much below 1 wt%[17].

The kinetics of cementite precipitation in TRIP steels depend on the carbon concentration of bainitic ferrite during the bainitic transformation[8]. Carbon partitioned from bainitic ferrite can either enrich the residual austenite or form carbides. Both processes can occur simultaneously, however, one process may dominate depending on the isothermal holding temperature and the alloy composition. It was noticed that in high silicon TRIP steels, carbide precipitation lags behind the formation of the bainitic ferrite and in fact, the microstructure of those silicon-rich alloys is carbide-free even after holding for several hours in the bainitic transformation region. Silicon is believed to oppose cementite formation from the residual austenite as reported by many authors, for example, as presented in the work of Bhadeshia and Edmonds[18]. The mechanism by which silicon retards cementite precipitation was proposed by Pichler *et al.*[19]. In their work, the suppression of cementite precipitation was suggested to be due to the very low silicon solubility in cementite.

It is well established that the composition of upper bainite cementite has a substitutional solute content which is close to or slightly higher than that of the alloy bulk composition[8]. Furthermore, in the work of Chance and Ridley concerning the upper bainite in an alloy of the composition Fe-0.81C-1.41Cr wt%, they found that the chromium partition coefficient (the ratio of chromium concentration in cementite to that of the austenite) was almost equal to unity[20]. Those findings suggest that the mechanism by which cementite grows is a displacive

mechanism[8]. This conclusion is interesting since the diffusion of the carbon partitioned from austenite must occur in the process of cementite precipitation. However, as reported by Bhadeshia, the diffusion involved in the process of cementite precipitation is of the interstitial not the substitutional solutes[8]. This leads to the conclusion that the diffusion of the interstitial solutes is still possible even at as low temperatures as -60 ºC. As such, the ratio of the concentration of iron to that of carbon remains constant throughout the steel which leads to that the carbon chemical potential achieves equality throughout the alloy. Therefore, cementite grows by a paraequilibrium transformation mechanism[8]. Many authors have published experimental evidence supporting the suggestion of the paraequilibrium displacive transformation mechanism[21-24]. As instance, for the case where cementite precipitates during martensite tempering by the paraequilibrium displacive transformation mechanism, according to the work of Babu *et al.*[25] using the atom probe technique, cementite particles had the same silicon concentration as that of the martensite, *i.e.* silicon has been trapped in the cementite during precipitation. As such, if cementite is forced to retain the silicon due to the paraequilibrium transformation mechanism, therefore, to large extent, the driving force for cementite precipitation is decreased which has the effect of retarding cementite precipitation[8].

However, some of the authors argued the possibility of substituting the silicon in conventional high-silicon TRIP-aided steels with, for example aluminium, which also not soluble in cementite[26]. Their results showed that aluminium can be a successful substitute to silicon. They reported achieving excellent mechanical properties and in particular; formability has been improved for a cold rolled C-Mn-Si TRIP steels with the silicon being partially substituted with aluminium. The purpose of adding an element which has no solubility in cementite, *i.e.* can be a potential substitute to silicon, is as an attempt to reduce the silicon content of conventional high-silicon TRIP-aided steels which causes some practical problems such as a poor surface finish[8,13] and for some applications; a galvanising problems[13,26].

The important factor to be considered while developing low-alloy TRIP-aided steels is to obtain a considerable amount of retained austenite in the alloy at room temperature and to manage to make it more stable and to transform progressively during plastic straining.

Chapter 2

Martensitic Transformation

Martensitic transformation is a solid-state diffusionless phase transformation. Only atomic movements over very small lengths less than the inter-atomic distance are required for the structural change to take place. Since diffusion does not occur, the chemical composition of the parent phase, austenite, and the product phase, martensite, is identical.

Martensitic transformation is also a displacive transformation hence it is accompanied by structural changes. Atoms or groups of atoms involved in the transformation process retain their neighbourhood relationships because of the co-ordinated atomic shifts[7].

Many diffusionless displacive phase transformations can be found in materials other than TRIP steels, which form a subset of a larger class of phase transformations sharing common features. Martensitic transformations can also be found in minerals, crystals and compounds which can, in principle, undergo a martensitic transformation provided that the rate of heating or cooling is sufficiently high so as to prevent the alternative diffusion-controlled transformation[14]. Therefore, rapid cooling of the steel from the austenitic region results in martensite formation, sometimes with retained austenite in the microstructure. The transformation process into martensite which is induced by relatively rapid cooling seems to be at random since the density of the formation of martensitic plates throughout the specimen appears to be independent from the austenite grain size[14]. As shown in Fig. 4, the newly formed martensitic plates have in general smaller size as the transformation process proceeds due to austenite partitioning caused by the previously transformed martensitic plates[27].

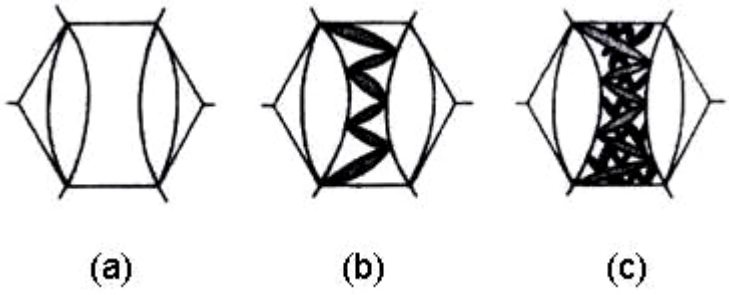

Fig. 4: The martensitic transformation within an austenite particle. As the transformation into martensite proceeds from (a) to (c), the size of newly formed martensitic plates decreases[27].

The transformation process from austenite to martensite can also be achieved by applying stress or strain rather than by rapid cooling. The main emphasis of this study is to investigate the strain-induced transformation behaviour of austenite which we believe still needs to be clarified, and in particular needs to be expressed quantitatively. Stress-assisted transformation of austenite has already been established, for example, as reviewed by Tamura[28] and Yu[29].

Applied mechanical loading can therefore contribute to the overall free energy necessary to start the transformation, via its introduction with the shape deformation[7]. It is therefore possible to nucleate martensite at temperatures above M_S as long as there is a sufficient mechanical driving force.

Patel and Cohen suggested that, above the M_S temperature, the change in the chemical driving force $\Delta G^{\gamma\to\alpha'}$ is linear as the temperature increases[30]. As shown in Fig. 5, it is expected that an increase in the mechanical driving force induced by external load (U') is necessary to aid the transformation at temperatures above M_S due to the decrease of the chemical driving force as temperature increases.

Fig. 5 represents the free energies of austenite and martensite as a function of temperature[28]. As shown in this figure, at a certain temperature T_0, both phases have exactly the same free

energy ($G_\gamma = G_{\alpha'}$). In the temperature range below T_0 martensite formation is thermodynamically favoured. However if the temperature is below that of T_0 and above M_S, no martensite is obtainable since the free energy difference between austenite and martensite has not yet reached the value of the critical chemical free energy $\Delta G_{M_S}^{\gamma\to\alpha'}$ for transformation to start. $\Delta G_{M_S}^{\gamma\to\alpha'}$ is the free energy difference between the two phases at M_S temperature. This is the exact free energy needed to allow for nucleation and also the stored energy of martensite. Nevertheless, martensite phase can form above M_S (for example at T_1) if there is an effect due to applied mechanical load (U'), such that its thermodynamic effect compensates for the difference between $\Delta G_{M_S}^{\gamma\to\alpha'}$ at M_S and $\Delta G_{T_1}^{\gamma\to\alpha'}$ at T_1 as shown in Fig. 5.

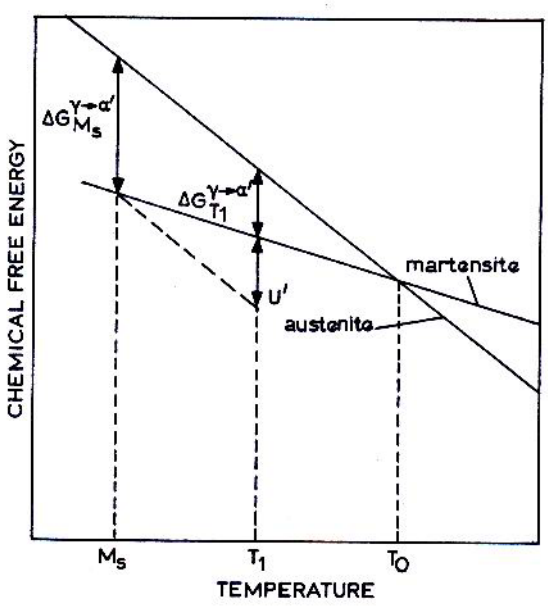

Fig. 5: Schematic illustration showing the free energy change of austenite and martensite as a function of temperature[28]. $\Delta G_{M_S}^{\gamma\to\alpha'}$ and $\Delta G_{T_1}^{\gamma\to\alpha'}$ are the free energy change due to transformation from austenite (γ) to martensite (α') at martensite start M_S and T_1 temperatures respectively. (U') is the thermodynamic effect of the applied mechanical load.

The martensitic transformation of interest in the present study fulfils the following features presented by Cohen[31]. These features are necessary and sufficient to define the martensitic transformation:

1) There must be a displacive lattice distortion involving a shape change with a dominant shear mechanism.
2) It is diffusionless.
3) Transformation kinetics must be dominated by sufficiently high shear-strain energy.

Chapter 3

Past models

Due to promising features such as the excellent strength-ductility balance and the competitive production cost of TRIP-aided steels, the need for an adequate general model able to predict the strain-induced transformation behaviour of austenite has been recognised. Many attempts have been proposed to meet such demand[32-37]. The main emphasis was however, the simulation of retained austenite stability.

Olson and Cohen proposed a model based on a theoretical analysis of the underlying transformation kinetics[33]. They argued the need for a model based on understanding the mechanism of the strain-induced nucleation. Strain-induced nucleation is different compared with stress-assisted nucleation. The former, strain-induced nucleation, introduces new nucleation sites formed by plastic deformation whereas in the case of stress-assisted nucleation, the effect of stress is to thermodynamically assist the transformation process of a previously formed nucleation site.

They began firstly by assuming that shear-band intersections in metastable austenite are primarily responsible for producing nucleation sites on which martensitic plates form. It is well established that shear-band intersections are effective nucleation sites for the strain-induced martensite[38-40]. Shear bands can either be in the form of ε' (hexagonal close-packed martensite), bundles of dense stacking-faults or mechanical twins. All of these forms are prompted by taking advantage of the low stacking-fault energy of the retained austenite[33]. In their treatment, they assumed that shear bands constitute a fraction of the plastic deformation in early stages of loading where strains are relatively small but as deformation proceeds, shear

bands hold a smaller fraction of plastic deformation hence shear-band-free volume is consumed.

The main idea of the model was to assume a constant consumption rate of shear-band-free austenitic volume per change in plastic strain. The analysis resulted in the following relationship:

$$f^{\alpha'} = 1 - \exp\left\{-\beta\left[1 - \exp\left(-\alpha\varepsilon\right)\right]^{n}\right\} \qquad [1]$$

where $f^{\alpha'}$ is volume fraction of martensite and ε is the plastic strain. As shown in equation 1, the transformation behaviour is determined by two temperature-dependent parameters α and β and an exponent n. α is sensitive to temperature through its dependence on stacking-fault energy and β is a probability term which defines the probability of an intersection to produce a nucleation site. This probability term β depends on temperature through the chemical driving force.

To validate the model, they fitted equation 1 to the experimental data of Angel[34] for 304 stainless steel. They assumed a value of $n = 4.5$ to fit adequately with the data.

Therefore the model represented by equation 1 lacks generality as there is a constant n with a specific value for each alloy being investigated.

However, this model, as it includes temperature-dependent parameters α and β, supports our assumption that in fact strain-induced transformation behaviour depends on the free energy available for transformation.

A different empirical approach was presented by Gerberich *et al*.[35]. In their model, a parabolic relationship was proposed to represent the strain-induced transformation behaviour of retained austenite as follows:

$$V_{\alpha'} = A_2 \varepsilon^{1/2} \qquad [2]$$

where $V_{\alpha'}$ is the martensite volume fraction and A_2 is a constant. As can be noticed, there is an absence of a term that would represent austenite volume fraction. This in effect assumes that no interactions take place between the transformed and the parent phase. The model, needs an empirical value of A_2 for each alloy, *i.e.* it lacks generality.

Guimarães proposed a similar exponential model as follows[37]:

$$V_{\alpha'} = 1 - \exp\left(-k\varepsilon^{Z}\right) \qquad [3]$$

where $k = 28$ and $Z = 3.7$ for Fe-Ni-C alloys. It is obvious that the given values of k and Z are exclusively applicable to the group of alloys studied.

Angel[34], Ludwigthusn and Berger[36] also proposed a quite similar approach. In their model, at constant temperature, the volume fraction of martensite transformed was assumed to be given as a function of the plastic strain (ε) as follows:

$$V_{\alpha'} = A_1 \varepsilon^{B} V_{\gamma} \qquad [4]$$

where V_{γ} is the initial volume fraction of austenite. A_1 and B are constants with a value of $B \approx 3$ for stainless steels. Compared with the previously mentioned models presented by

Gerberich *et al.*[35] and that of Guimarães[37], this model takes into account possible interactions between both retained austenite and martensite as plastic deformation proceeds. However, the constants in equation 4 are alloy-dependent and therefore, the model is not a general model for all TRIP-aided steel alloys.

Sugimoto *et al.*[32] proposed a relationship that gives the amount of retained austenite transformed to martensite as a function of the applied plastic strain:

$$\ln\{V_\gamma^0\} - \ln\{V_\gamma\} = k\varepsilon \qquad [5]$$

where V_γ^0 is the initial volume fraction of austenite, V_γ is volume fraction of austenite and k is a constant. Equation 5 has been used widely to investigate the strain-induced transformation behaviour at deforming temperatures above M_S. This relationship was originally obtained by fitting to a definite set of experimental data of certain alloys, it expresses the transformation behaviour of the corresponding alloys. This is shown in Fig. 6 where the value of k varies for different alloys at the same deformation temperature.

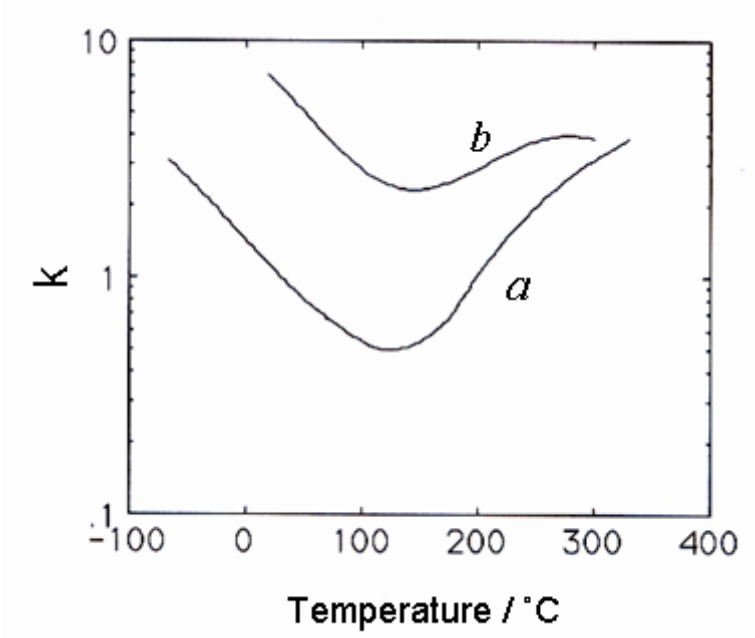

Fig. 6: A plot of values of the coefficient in equation 5, k, versus tensile-testing temperature for steel (a) with $M_S = -61$ ˚C and steel (b) with $M_S = -7$ ˚C. Experimental data are of Sugimoto *et al.*[32]

As represented in equation 5, the k-value is crucial and actually determines retained austenite stability hence as k-value decreases the retained austenite becomes more stable and resistant to transformation.

As shown in Fig. 3, Sugimoto *et al.*[32] proved experimentally that there is a strong dependence between k-value and deformation temperature, that is in our view, rather free energy dependent.

Chapter 4

Theory

It is proposed here that the main parameter for describing the strain-induced transformation behaviour of retained austenite should be the free energy available for transformation. In other words, the constant k in equation 5 should include the free energy $\Delta G^{\alpha\gamma}$.

The free energy change must of course be negative in order for transformation to occur. To express the magnitude of $\Delta G^{\gamma\alpha}$, we write $\Delta G^{\alpha\gamma} = -\Delta G^{\gamma\alpha}$.

The free energy term naturally includes the effects of both the chemical composition and tensile-testing temperature; both of these variables influence the thermodynamic stabilities of the austenite and ferrite. It is expected that as the deformation temperature increases[32], or at higher manganese or carbon concentrations[1,13], the austenite becomes less sensitive to plastic strain.

The temperature range of interest in this study is above the M_S temperature and up to about 473 K. Within this temperature range, according to Sugimoto *et al.*[32], k decreases as the temperature increases. It is argued here that the minimum value of k is zero since no amount of plastic strain can induce transformation when the deformation temperature exceeds M_d.

Chapter 5

The model

5.1 The First model

To develop the theory, it is necessary to consider how equation 5 might be derived. One assumption is that the change in martensite volume fraction $dV_{\alpha'}$ per unit change of plastic strain $d\varepsilon$ might be expressed as a function of the volume fraction of the untransformed austenite V_γ as follows:

$$\frac{dV_{\alpha'}}{d\varepsilon} = k\, V_\gamma \qquad [6]$$

This equation essentially states that the *rate* of transformation depends on the amount of parent phase, and hence is considered to be reasonable. Since the volume fraction of martensite is given by $V_{\alpha'} = V_\gamma^0 - V_\gamma$ where V_γ^0 is the initial volume fraction of austenite at zero strain, by substituting into equation 6 and integrating, equation 6 can be written as equation 5 which was suggested by Sugimoto *et al.*[32]

Since it is proposed here that k in equation 5 has a strong dependence on the free energy available for transformation, then k can be re-written as $k = k_1 \Delta G^{\alpha\gamma}$ in which case equation 6 becomes:

$$\ln\{V_\gamma^0\} - \ln\{V_\gamma\} = k_1 \Delta G^{\alpha\gamma} \varepsilon \qquad [7]$$

To test this relationship, free energy calculations were carried out using MTDATA with the NPL-plus database for steels[41].

To validate the model given by equation 7, experimental data were collected from the literature[1,13,15,32,42-44]. the chemical composition and temperature ranges covered by the data are given in table 1.

C_γ	$\overline{C}$	*Mn*	*Si*	*Cr*	*Ni*	Temperature/K
0.73-1.83	0.13-0.60	0.80-1.66	0.38-2.00	0-0.17	0-0.16	293-423

Table 1: Chemical composition and temperature ranges of steels investigated. Compositions are in wt%. C_γ is the carbon content in austenite and $\overline{C}$ is the average carbon concentration in steel.

The free energies were calculated using estimated chemical composition of austenite[45]. It was assumed that during isothermal holding in the bainite transformation temperature region, except for carbon, no diffusion takes place. the carbon concentration in austenite for each alloy was given in the published literature, based on measurements made using the X-ray diffraction technique.

Given the deformation temperature at which the tensile test was carried out, it was possible to estimate the exact value of the free energy necessary for transformation to start.

By plotting all the accumulated values of $\ln\{V_\gamma^0\} - \ln\{V_\gamma\}$ versus $\Delta G^{\alpha\gamma}\varepsilon$ for all investigated alloys, it was possible to calculate a best-fit value of $k_1 = 0.002017$ mol J^{-1}. Fig. 4 (a) gives the measured versus calculated volume fractions of retained austenite of the entire dataset based on published measurements.

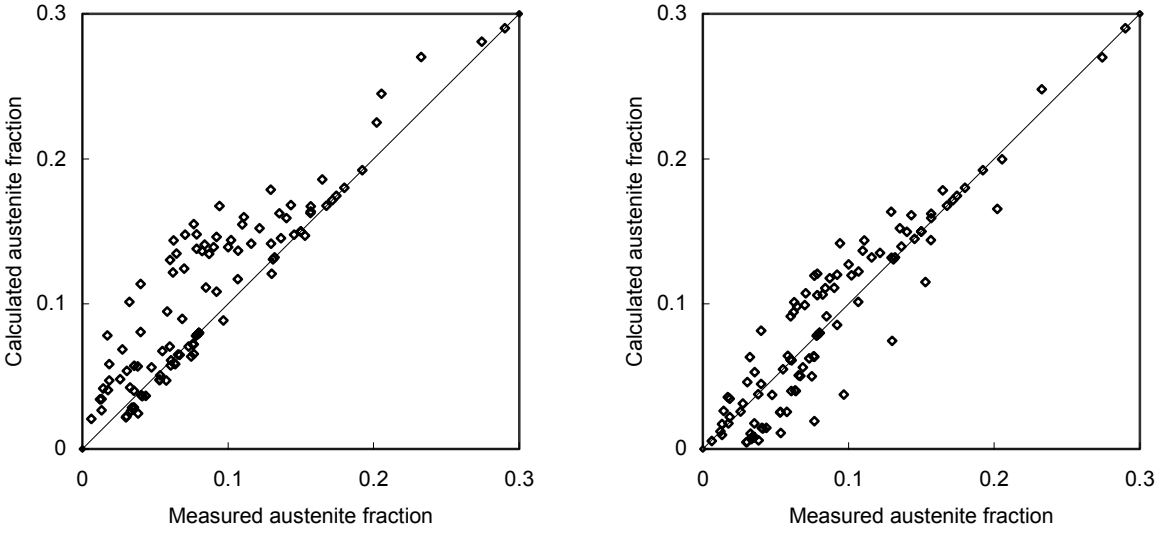

(a) Analysis based on $k_1 = 0.002017$ mol J^{-1}.

(b) Analysis based on $k_1 = 0.00446$ mol J^{-1}.

Fig. 7: Plot of the analysis based on equation 7. The line indicated represents the ideal case where both predicted and measured values are identical. (a) With correlation coefficient 0.91 and standard error ± 0.026. (b) With correlation coefficient 0.93 and standard error ± 0.023.

As shown in Fig. 7 (a), the agreement with the experimentally measured austenite volume fractions was reasonable given the range of temperatures and chemical compositions involved. However, the model seems to systematically overestimate the retained austenite content.

There was a difficulty, or in other words, a logical error in the technique used to process the data. Since all data were analysed from the variety of steels were analysed together as a single set, and since the number of data associated with each alloy was different, alloys with larger quantities of data are expected to bias the value of k_1. To overcome this difficulty, individual alloys were analysed separately and an average k_1 was obtained from the resulting set of values. The average k_1 was in this way found to be $k_1 = 0.00446$ mol J^{-1}. This procedure gives equal prominence to each experiment and therefore leads to a better representation of

the phenomenon being investigated. As shown in Fig. 7 (b), using the new value of k_1 gives better results with a higher correlation coefficient and lower standard error compared with the previous value of k_1.

5.2 Hydrostatic Pressure

The influence of hydrostatic pressure has in the past been introduced[46] through a modification of the constant k in equation 5:

$$\ln\{V_\gamma^0\} - \ln\{V_\gamma\} = (k - \beta P)\varepsilon \qquad [8]$$

where β is an empirical constant and P is the hydrostatic pressure. According to equation 8, the effect of hydrostatic pressure is to reduce the rate of the strain-induced transformation of austenite. This was expected from the volume expansion accompany any martensite transformation in steels, as previously reported by Patel and Cohen[30].

The free energy of transformation at ambient pressure $\Delta G^{\gamma\alpha}\{1\}$ can be expressed as a function of pressure as follows[8]:

$$\Delta G^{\gamma\alpha}\{P\} - \Delta G^{\gamma\alpha}\{1\} = \int_1^P \Delta V_m dP' \qquad [9]$$

where ΔV_m is the change in the molar volume upon transformation, equivalent to the term β in equation 7 provided that the difference in molar volumes remains constant over the pressure range of interest.

Therefore, the approach presented by Pyshmintsev *et al.*[46] is equivalent to our approach embodied in equation 7.

5.3 Chemical Composition and Temperature

Changing the chemical composition of TRIP-aided steels, particularly carbon and manganese concentration, is expected to influence the stability of retained austenite[1,13]. Using the model summarised by equation 7, it is possible to investigate the effect of the chemical composition and tensile-testing temperature on the strain-induced transformation behaviour.

It is interesting that the effect of any new alloying element (for example, cobalt), which has not been studied previously, can be calculated through the free energy term $\Delta G^{\alpha\gamma}$, which in turn can be calculated using MTDATA.

To put the model based on equation 7 with a value of $k_1 = 0.00446$ mol J^{-1} into practice, the retained austenite content of a hypothetical alloy of the base composition Fe-xC-xMn-2Si wt% with a range of carbon and manganese concentrations was studied. This is to investigate the effect of varying carbon and manganese concentration at different deformation temperatures on the transformation behaviour of retained austenite during straining. Initial volume fraction of the retained austenite has been calculated via the equation:

$$C_\gamma = \frac{\overline{C} - 0.03(1 - V_\gamma^0)}{V_\gamma^0} \qquad [10]$$

assuming that carbon content in ferrite is 0.03 wt%.

Fig. 8,9 shows the effect of varying manganese concentration at different working temperatures for austenite carbon content $C_\gamma = 0.6$ and $C_\gamma = 1.2$ wt%.

As shown in Fig. 8 and Fig. 9, varying the chemical composition has a great effect on austenite stability. It is interesting that the strain-induced transformation behaviour of

austenite is less sensitive to the change in manganese concentration compared with the change in carbon concentration.

Doubling the carbon content in retained austenite resulted in much higher austenite stability compared with the case when manganese concentration has increased five times from 0.5 wt% to 2.5 wt%. The reason for this is of course the effect of carbon and manganese on the free energy $\Delta G^{\alpha\gamma}$.

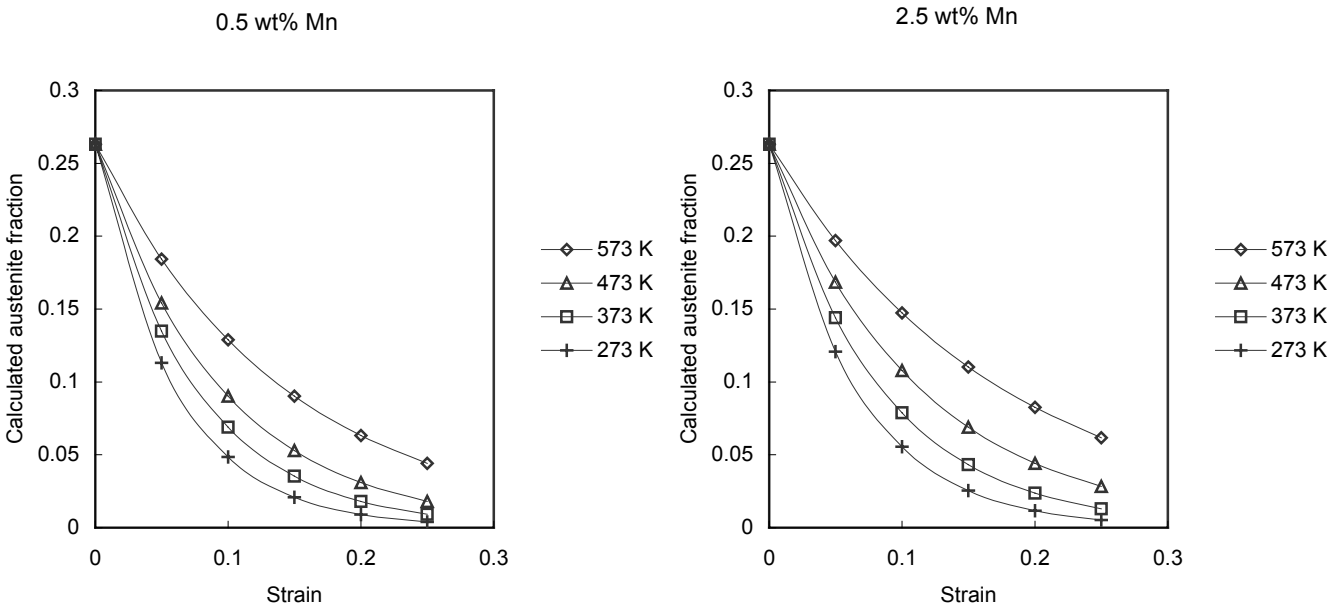

Fig. 8: Example calculations using equation 7 and $k_1 = 0.00446$ mol J^{-1} for a steel of base composition Fe-Mn-2Si wt% and $C_\gamma = 0.6$ wt% with $V_\gamma^0 = 0.2632$.

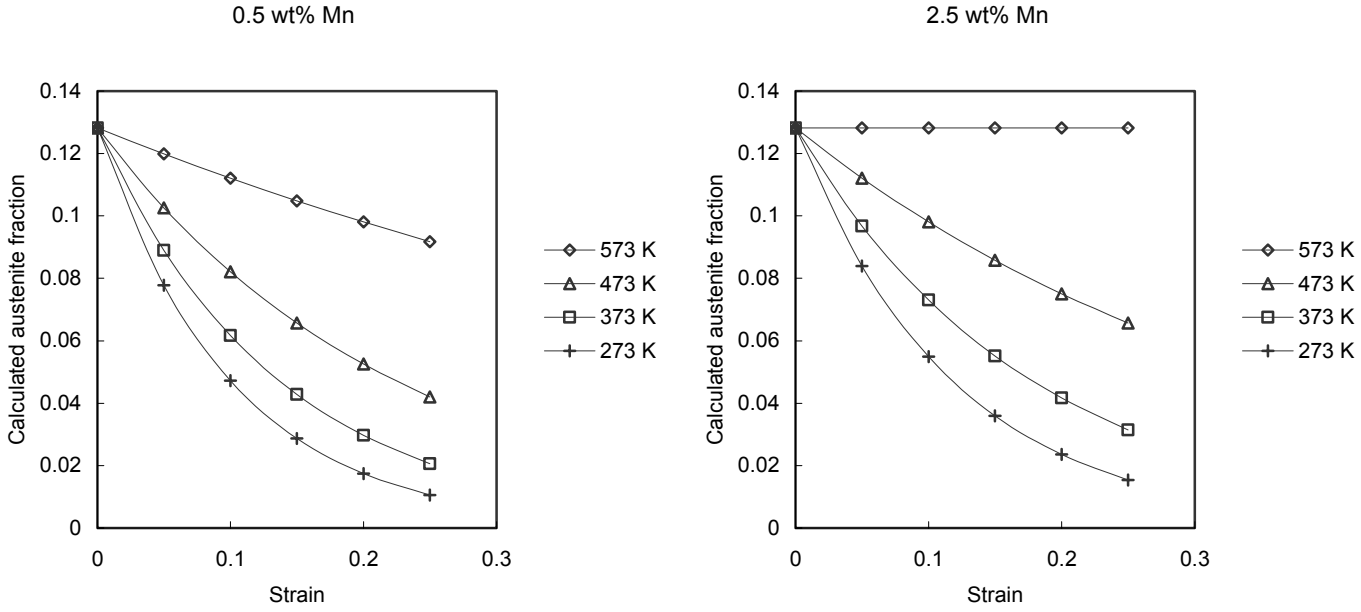

Fig. 9: Example calculations using equation 7 and $k_1 = 0.00446$ mol J^{-1} for a steel of base composition Fe-Mn-2Si wt% and $C_\gamma = 1.2$ wt% with $V_\gamma^0 = 0.1282$.

Fig. 10 represents the free energy term $\Delta G^{\alpha\gamma}$ calculated using MTDATA for the studied hypothetical alloy versus temperature. The graph shows that the free energy $\Delta G^{\alpha\gamma}$ decreases linearly with the increase of the tensile-testing temperature and or the austenite solute content. However, at a certain working temperature, the free energy calculated is more sensitive to the change in the carbon content compared with manganese. This might have an effect on the processing route to be followed in the context of designing TRIP-aided steels. It is beneficial to enrich retained austenite with carbon by applying a longer holding times in the bainite transformation temperature region[1] or adding more silicon[18,47] rather than to add more manganese to the alloy in an attempt to increase austenite stability. Furthermore, reducing the manganese concentration in the alloy has the beneficial effect of ensuring obtaining a sufficient volume fraction of bainite in the microstructure and consequently high tensile strength levels.

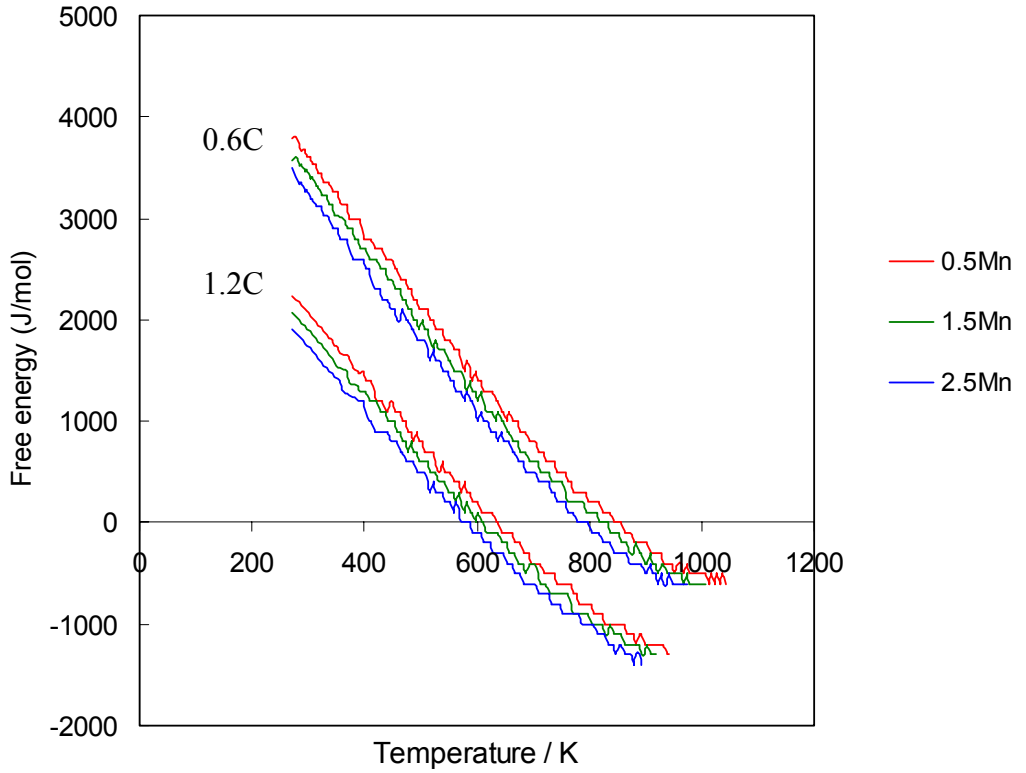

Fig. 10: A plot of the calculated free energy $\Delta G^{\alpha\gamma}$ versus temperature of a hypothetical alloy with the base composition Fe-Mn-2Si wt%. C_γ =0.6 and 1.2 wt%, manganese concentration range is 0.5-2.5 wt%.

It is clear that straining at higher temperatures results in increased austenite stability. At a sufficiently high temperature, transformation is completely suppressed as shown in Fig. 9. This temperature corresponds to the M_d temperature.

Fig. 11 shows three dimensional plots of the effect of varying carbon and manganese concentrations at the temperature range 273-573 K on the strain-induced transformation behaviour of retained austenite using the same hypothetical alloy of the base composition Fe-xC-xMn-2Si wt%.

Fig. 11 is calculated using the model summarised by equation 7 with k_1 = 0.00446 mol J^{-1}.

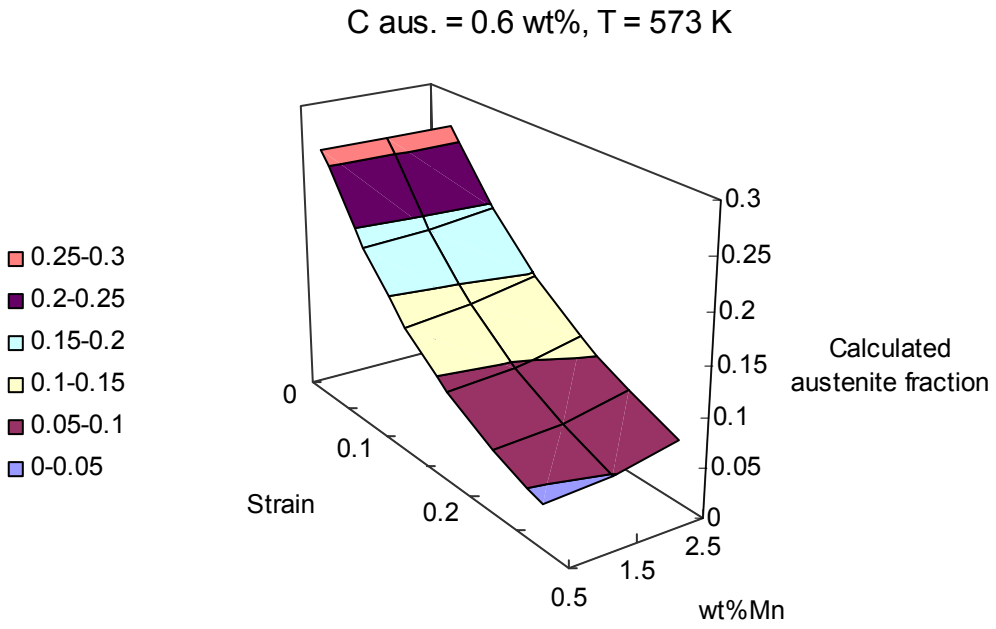
C aus. = 0.6 wt%, T = 573 K
0.25-0.3
0.2-0.25
0.15-0.2
0.1-0.15
0.05-0.1
0-0.05
0
0.1
0.2
Strain
0.5
1.5
2.5
wt%Mn
0
0.05
0.1
0.15
0.2
0.25
0.3
Calculated
austenite fraction

(a)

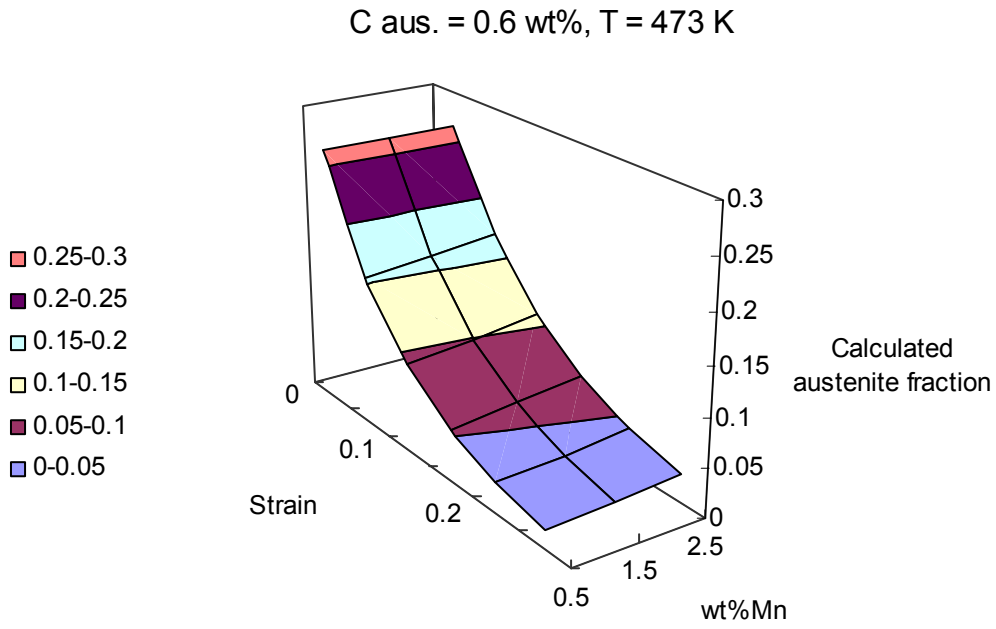
C aus. = 0.6 wt%, T = 473 K
0.25-0.3
0.2-0.25
0.15-0.2
0.1-0.15
0.05-0.1
0-0.05
0
0.1
0.2
Strain
0.5
1.5
2.5
wt%Mn
0
0.05
0.1
0.15
0.2
0.25
0.3
Calculated
austenite fraction

(b)

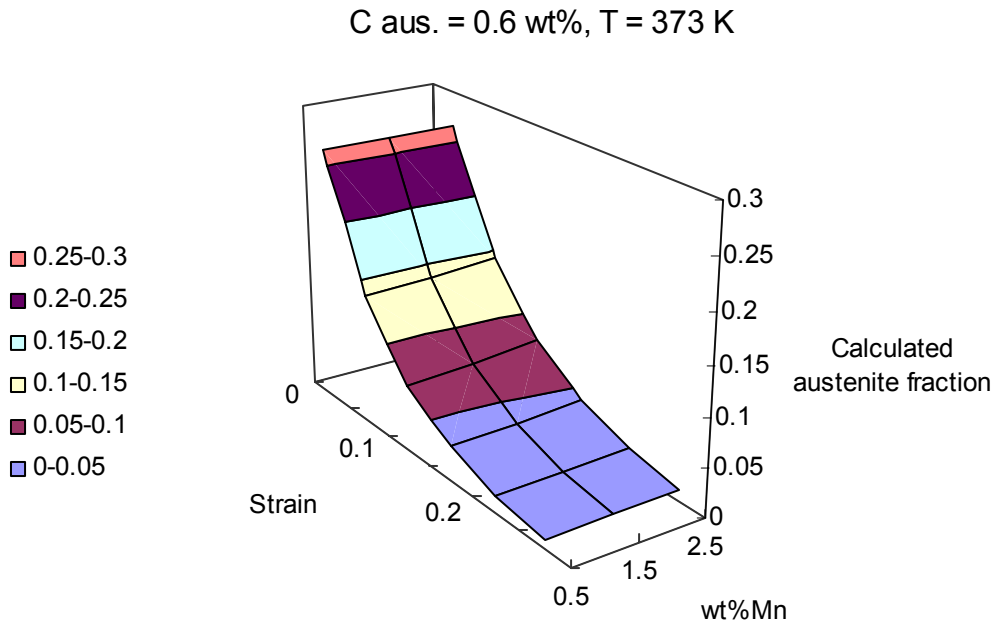
C aus. = 0.6 wt%, T = 373 K
0.25-0.3
0.2-0.25
0.15-0.2
0.1-0.15
0.05-0.1
0-0.05
Strain
0
0.1
0.2
0.5
1.5
2.5
wt%Mn
0
0.05
0.1
0.15
0.2
0.25
0.3
Calculated
austenite fraction

(c)

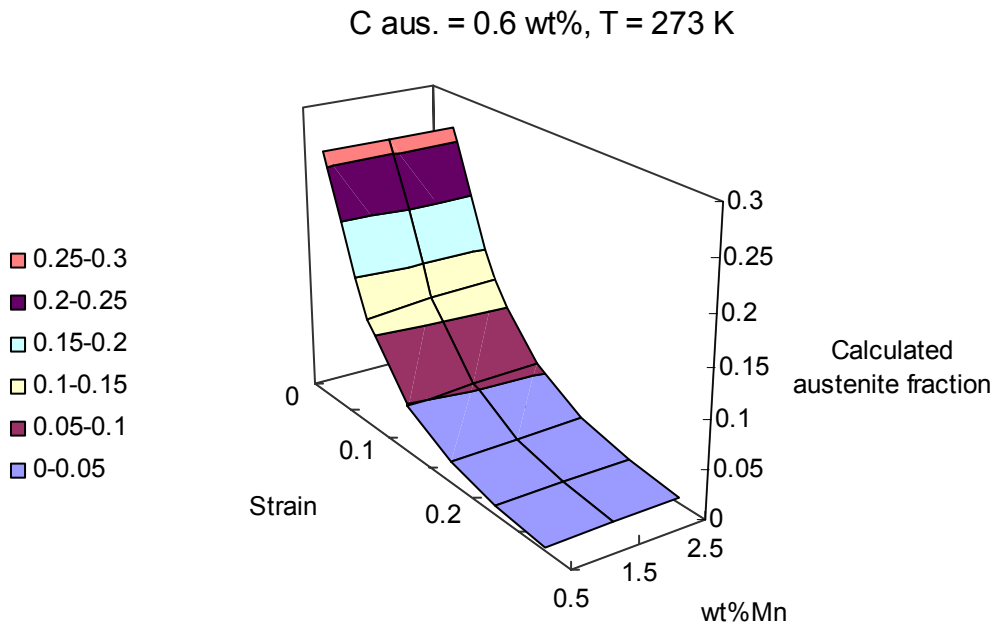
C aus. = 0.6 wt%, T = 273 K
0.25-0.3
0.2-0.25
0.15-0.2
0.1-0.15
0.05-0.1
0-0.05
Strain
0
0.1
0.2
0.5
1.5
2.5
wt%Mn
0
0.05
0.1
0.15
0.2
0.25
0.3
Calculated
austenite fraction

(d)

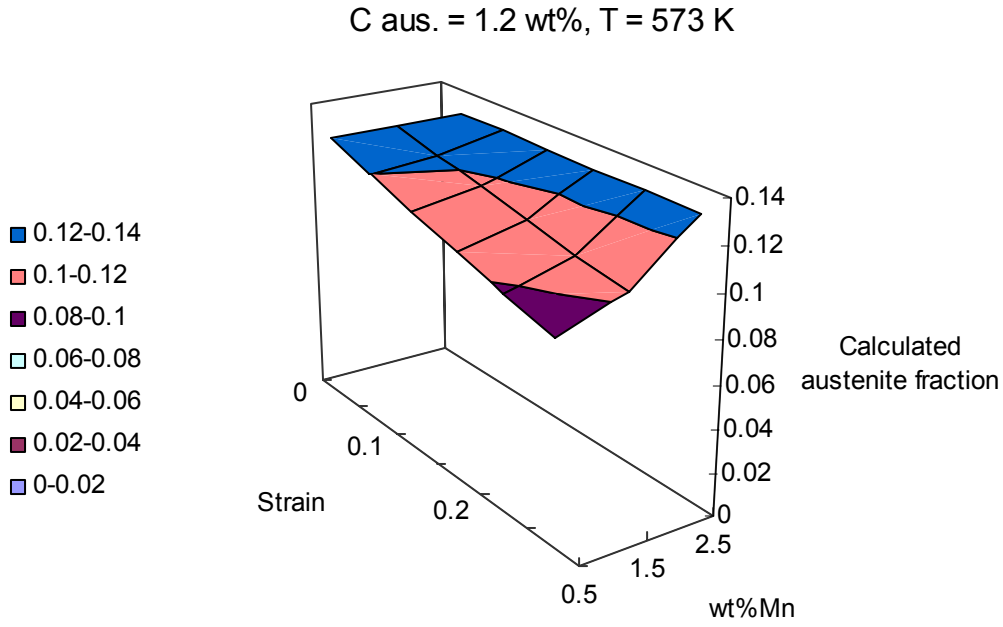
C aus. = 1.2 wt%, T = 573 K
0.12-0.14
0.1-0.12
0.08-0.1
0.06-0.08
0.04-0.06
0.02-0.04
0-0.02
Strain
0
0.1
0.2
wt%Mn
0.5
1.5
2.5
Calculated
austenite fraction
0
0.02
0.04
0.06
0.08
0.1
0.12
0.14

(e)

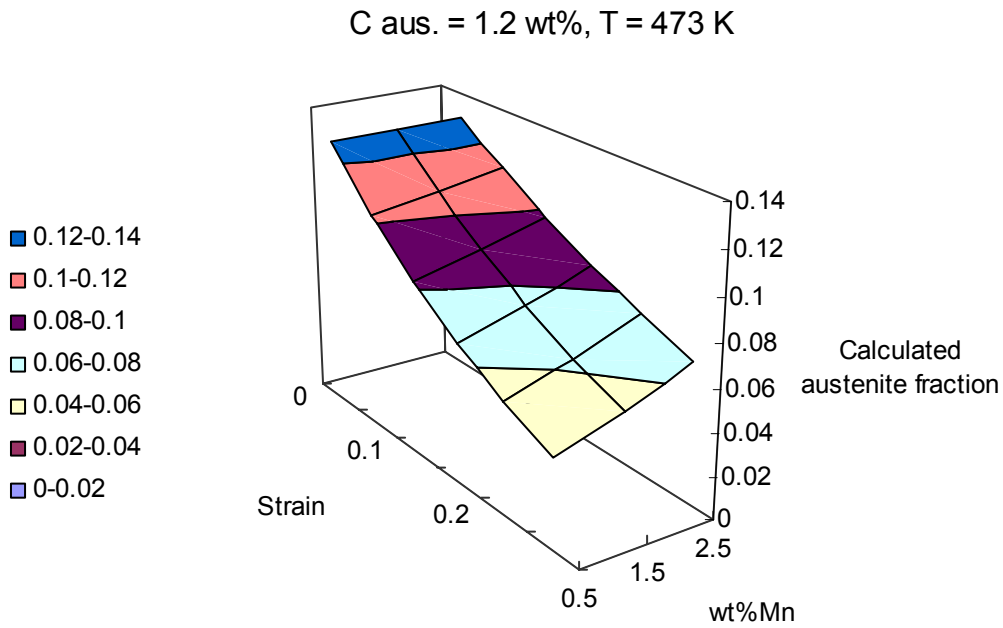
C aus. = 1.2 wt%, T = 473 K
0.12-0.14
0.1-0.12
0.08-0.1
0.06-0.08
0.04-0.06
0.02-0.04
0-0.02
Strain
0
0.1
0.2
wt%Mn
0.5
1.5
2.5
Calculated
austenite fraction
0
0.02
0.04
0.06
0.08
0.1
0.12
0.14

(f)

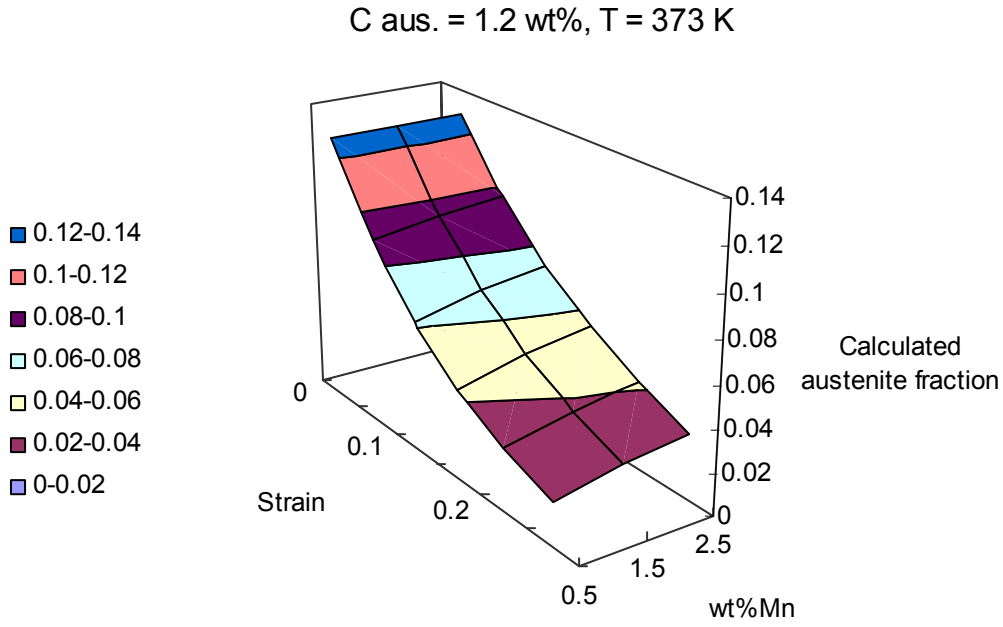

(g)

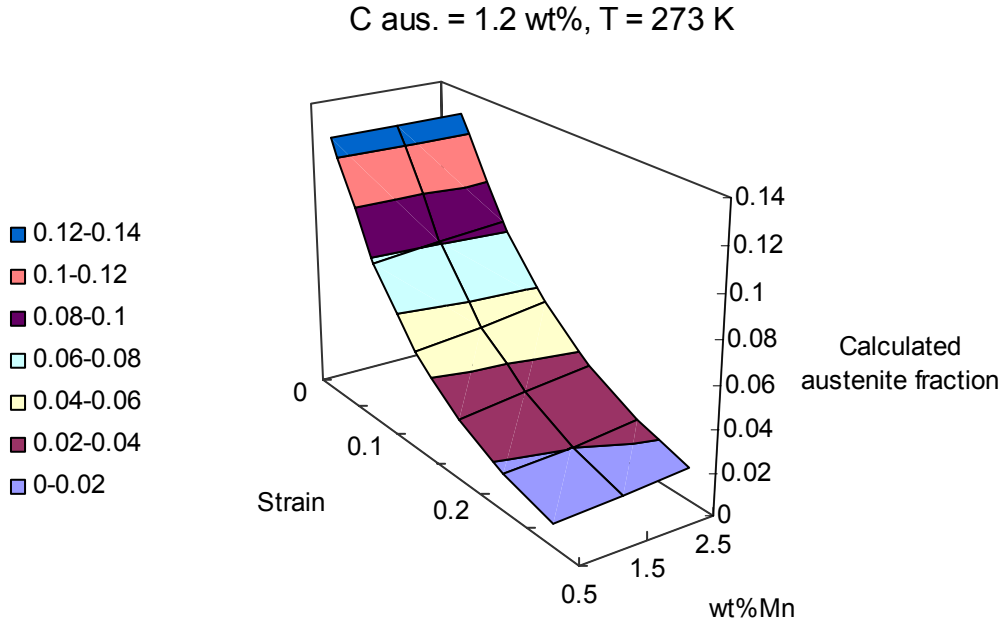

(h)

Fig. 11: Example calculations using equation 7 with k_1 = 0.00446 mol J^{-1}. A hypothetical alloy of the base composition Fe-Mn-2Si wt% has been used. "C aus." is the austenite carbon content (C_γ). For figures (a) to (d), V_γ^0 = 0.2632 and for (e) to (h), V_γ^0 =0.1282.

Chapter 6

Alternative model

Olson and Cohen proposed that strain-induced martensitic transformation is essentially controlled by the formation of nucleation sites due to shear-band intersections[33]. Each nucleus may then transform into a plate of a specified volume $\overline{V}$. Singh and Bhadeshia reported that the plate thickness decreases as $\Delta G^{\alpha\gamma}$ increases[48]. Therefore, at larger driving forces, the volume of a martensitic plate is expected to decrease, leaving more austenite untransformed. This variation in $\overline{V}$ has not been taken into account when driving equation 7.

According to Singh and Bhadeshia[48], the relationship between martensitic plate thickness and free energy $\Delta G^{\alpha\gamma}$ is almost linear over the range of parameters they studied, so that it can be expressed using an equation of the form:

$$\overline{V} = \overline{V}_o + \frac{\partial \overline{V}}{\partial(\Delta G^{\alpha\gamma})} \times \Delta G^{\alpha\gamma} \qquad [11]$$

where $\overline{V}_o$ (the initial plate volume) and $\frac{\partial \overline{V}}{\partial(\Delta G^{\alpha\gamma})}$ is a constant. Hence the effect of strain in equation 7 is proportional to $\overline{V}$. A more detailed expression of the transformation behaviour can therefore be given as follows:

$$\ln\{V_\gamma^o\} - \ln\{V_\gamma\} = k_2 \overline{V} \Delta G^{\alpha\gamma} \varepsilon \qquad [12]$$

Substituting into equation 12 with the value of $\overline{V}$ given by equation 11, gives:

$$\ln\{V_\gamma^o\} - \ln\{V_\gamma\} = k_2\left[\overline{V}_o + \frac{\partial \overline{V}}{\partial(\Delta G^{\alpha\gamma})}\Delta G^{\alpha\gamma}\right]\Delta G^{\alpha\gamma}\varepsilon$$

$$= \underbrace{\left[k_2\overline{V}_o\Delta G^{\alpha\gamma} + k_2\frac{\partial \overline{V}}{\partial(\Delta G^{\alpha\gamma})}(\Delta G^{\alpha\gamma})^2\right]}_{\phi}\varepsilon \qquad [13]$$

For a given alloy i deformed at a certain temperature, a plot of $\ln\{V_\gamma^0\} - \ln\{V_\gamma\}$ versus ε gives a value of ϕ_i.

Using all accumulated values of $\frac{\phi_i}{\Delta G_i^{\alpha\gamma}}$ and $\Delta G_i^{\alpha\gamma}$ of their respective alloys, and by using the following linear equation:

$$\frac{\phi_i}{\Delta G_i^{\alpha\gamma}} = \underbrace{k_2\overline{V}_0}_{k_3} + \underbrace{k_2\frac{\partial \overline{V}}{\partial(\Delta G^{\alpha\gamma})}}_{k_4}\Delta G_i^{\alpha\gamma} \qquad [14]$$

all the unknowns in equation 13 can be solved, giving $k_3 = 0.008478$ mol J^{-1} and $k_4 = -2.42\times10^{-6}$ mol J^{-1}.

Results obtained using this alternative model showed excellent agreement with experimental data with a standard error of ± 0.015 as shown in Fig. 12.

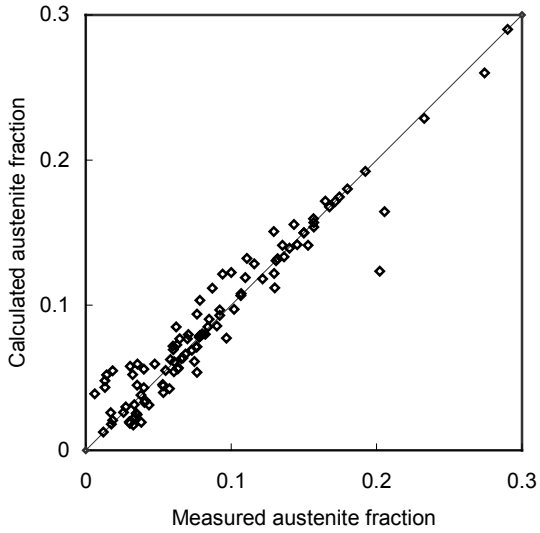

Fig. 12: Plot of the predicted versus measured austenite volume fractions using the alternative model presented by equation 13. The line indicated represents the ideal case where both predicted and measured values are identical. The correlation coefficient is 0.96 with a standard error ± 0.015.

Fig. 12 shows excellent agreement with experimental data hence the alternative model has a better correlation coefficient and smaller standard error compared with the model given by equation 7.

However, it is important to emphasise that this alternative model, although it indicates the role of martensite plate size and furthermore, it is more accurate compared with the previous model, it is limited to free energy values less than about 2500 J mol^{-1}. In other words, at relatively high free energies, the martensitic plate thickness approaches zero. This is because the alternative model was basically based on the idea of introducing $\overline{V}$ effect through making use of the linear equation 11, which is essentially empirical.

Using the alternative model, some calculations were carried out for the same hypothetical alloy used to produce the results shown in Fig. 8 and Fig. 9. As shown in Fig. 13, there were some illogical results for example reporting the austenite volume fraction as it increases with

strain. this can be explained as the martensitic plate size becomes negative at relatively high energy values. Hence at free energy values over about 2500 J mol^{-1}, the alternative model given by equation 13 seems not to behave correctly. This can be explained since at relatively high free energy $\Delta G^{\alpha\gamma}$ the plate size becomes negative. To indicate the effect of the value of calculated free energy on the degree of prediction accuracy, Fig. 14 and Fig. 15 show a general comparison between both models proposed in this study and the experimental data of two alloys[1,43]. The selection of these specific alloys was based on their calculated free energy which was 510 J mol^{-1} for the alloy presented in Fig. 14 and 3160 J mol^{-1} for the alloy presented in Fig. 15. These two values of the free energy were the minimum and the maximum values calculated.

As shown in Fig. 14, where the free energy was relatively low, the alternative model gives better predictions. On the other hand, for the case where the free energy was relatively high, the transformation behaviour was better described using the model presented by equation 7.

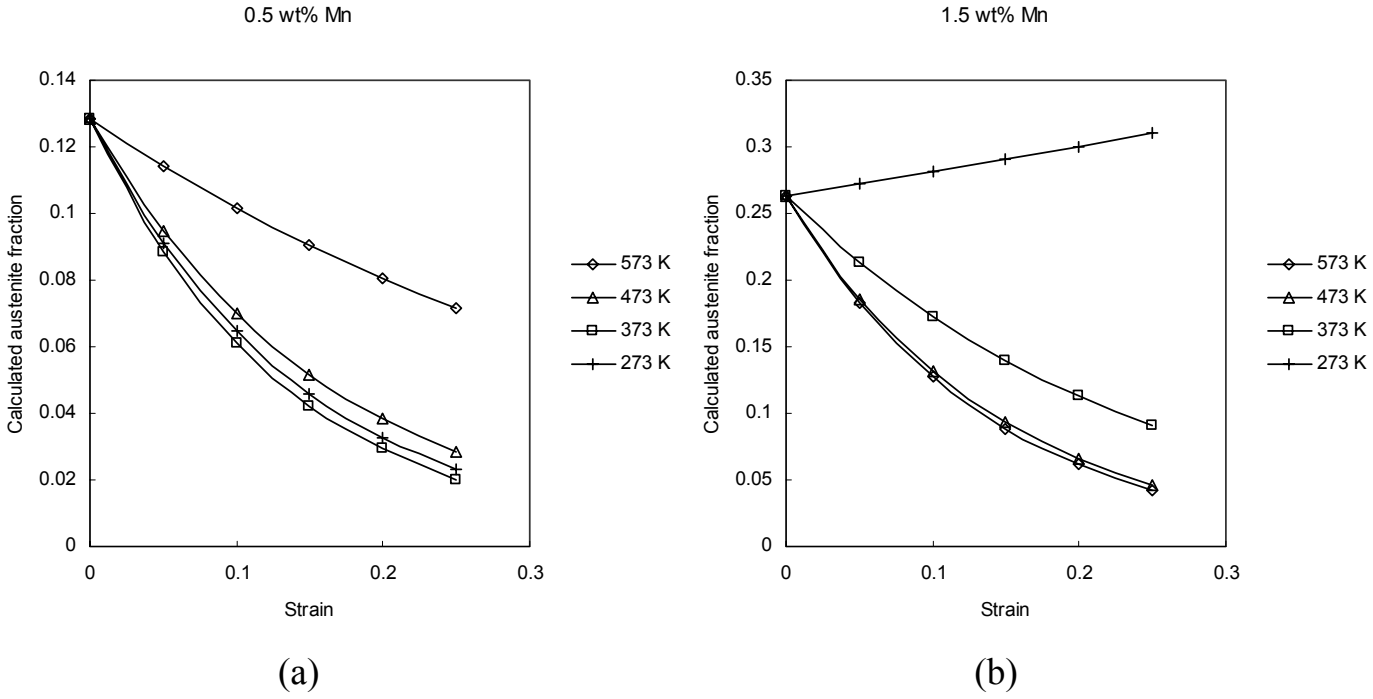

Fig. 13: Example of calculations carried out using the alternative model for a steel of base composition Fe-Mn-2Si wt%. (a) austenite carbon content is 1.2 wt% with $V_\gamma^0 = 0.1282$. (b) austenite carbon content is 0.6 wt% with $V_\gamma^0 = 0.2632$.

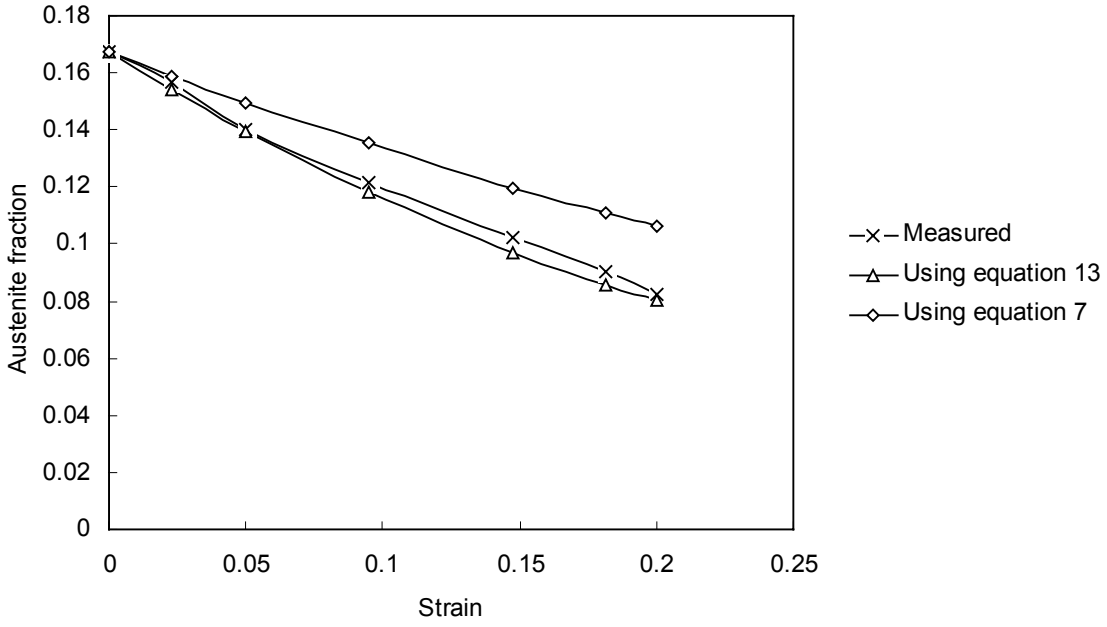

Fig. 14: A plot representing measured and calculated values of austenite content versus strain[1]. Tensile-testing was carried out at room temperature. Calculated free energy $\Delta G^{\alpha\gamma}$ was 510 J mol^{-1} for an alloy of the composition Fe-1.53Si-0.83Mn wt%. C_γ = 1.83 wt%.

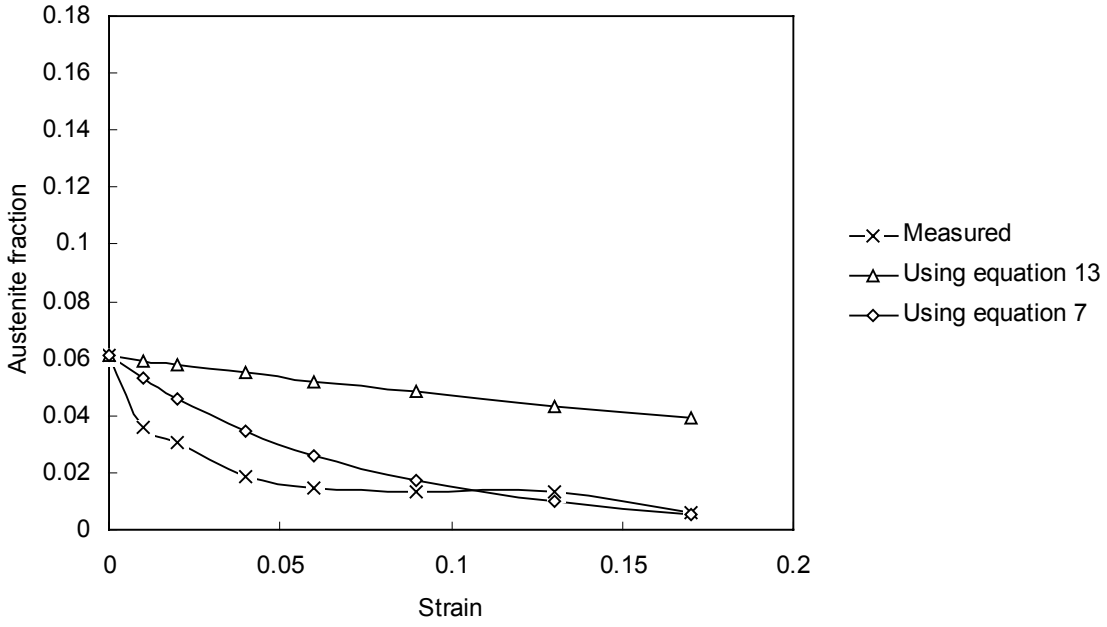

Fig. 15: A plot representing measured and calculated values of austenite content versus strain[43]. Tensile-testing was carried out at room temperature. Calculated free energy $\Delta G^{\alpha\gamma}$ was 3160 J mol^{-1} for an alloy of the composition Fe-0.38Si-1.3Mn wt%. C_γ = 0.73 wt%.

Chapter 7

Summary and Future Work

In TRIP-aided steels, strain-induced transformation of austenite to martensite occurs during deformation and reported to be beneficial to the total elongation and consequently ductility. However, controlling the transformation process is crucial because the premature transformation of austenite during the early stage of deformation is detrimental to ductility. Therefore, the aim of many studies carried out in the past was to make the austenite retained and less sensitive to plastic deformation. Many experiments have been carried out to study methods to stabilise the austenite. It is evident that a model for strain-induced transformation of austenite as a function of chemical composition, strain and temperature would be extremely useful in the design of TRIP-aided steels. However, almost all published models are essentially empirical in the sense that they are limited to certain named ranges of applicability. In the present work a model has been developed which has much greater generality, via the dependence of transformation on the thermodynamic driving force, *i.e.* the free energy $\Delta G^{\gamma\alpha}$. Therefore, it has been possible to consider other physical parameters rather than just plastic strain.

The hydrostatic pressure effect[46] can also be considered through altering the free energy value as shown in equations 7-9. It is expected that hydrostatic pressure decreases the transformation rate by opposing volume expansion accompanied by the transformation.

One of the most exciting outcomes is the ability to calculate the M_d temperature for any alloy given its chemical composition. This has not been possible before. The M_d temperature showed a strong dependence on alloy chemical composition.

Unlike previously proposed models[32-37], it has been possible to propose a general model that is alloy-independent, *i.e.* uses universal values for fitted constants, without actually increasing the number of fitting parameters. Both proposed models exhibit good correlation with experimental data although the apparent limitation exists in case of the *alternative* model. The limitation arises because of the empirical representation of the volume per plate of martensite. The applicability of the alternative model is restricted to $\Delta G^{\alpha\gamma}$ values no more than about 2500 J mol^{-1}. It is important to consider in future research the empirical equation 11 as an attempt to drive an equation which might be capable of describing the more general relationship between the martensitic plate size and the free energy. It is possible to investigate the effect of adding other alloying elements on the stability of the retained austenite. This is to find a combination of alloying elements to provide with the required mechanical properties and can be successfully used as a partial substitution to silicon. Furthermore, an adequate combination of alloying elements may be used so as to lower the bulk carbon concentration of TRIP steels without loss of austenite stability. As such, the well known practical problems, for example, welding of high-carbon steels, can be, to large extent, reduced. The alternative model can also be improved by taking into account the austenite grain size and morphology.

APPENDIX

MTDATA

In this study, thermodynamic calculations were carried out using MTDATA (Metallurgical and Thermochemical DATAbank) package. It predicts phases and their compositions at chemical equilibrium in complex multi-component multi-phase systems using critically assessed thermodynamic data based on simpler sub-systems (SGTE-databases). Some phase transformations occur such that only some elements can partition. This is the case as in, for example, bainitic transformation in which only carbon partitions whilst other substitutional elements maintain their relative amounts in different phases. In MTDATA it is also possible to set a paraequilibrium conditions by enforcing the program to compute the equilibrium state under these constraints. This package uses reliable Gibbs free energy minimisation algorithm (MULTIPHASE STAGE_1) to guarantee that free energy has been reduced in calculation.

Gibbs free energy of a random substitutional solution can be written as:

$$G = \sum_i x_i G_i^0 + RT \sum_i x_i \ln x_i + G_{mix}^{excess} \qquad [1]$$

where G_i^0 is the contribution due to the pure components, G_{mix}^{excess} is the excess Gibbs free energy of mixing, or in other words, the deviation from the ideality. R is the gas constant and x_i is the atomic fraction of component i. For a regular solution, the excess Gibbs free energy can be described as:

$$G_{mix}^{excess} = \sum_i \sum_{j \rangle i} x_i x_j \omega_{ij} \qquad [2]$$

where ω_{ij} is a temperature dependent parameter. However, equation 2 assumes no composition dependency. Kaufman and Berstein have introduced a linear composition dependency, therefore, the excess Gibbs free energy can be written as:

$$G_{mix}^{excess} = \sum_{i} \sum_{j \rangle i} x_i x_j (\omega_{ij}^{i} x_i + \omega_{ij}^{j} x_j) \qquad [3]$$

Equation 3 can be generalised to consider any composition dependency as presented by the Redlich-Kister power series:

$$G_{mix}^{excess} = \sum_{i} \sum_{j \rangle i} x_i x_j \sum_{\upsilon} \omega_{ij}^{\upsilon} (x_i - x_j)^{\upsilon} \qquad [4]$$

ω in SGTE thermodynamic databases is summarised as follows:

$$\omega = A + BT + CT \ln T + DT^2 \qquad [5]$$

and the coefficients associated with each ω_{ij}^{υ} are stored. However, unlike the case when components in a phase can mix randomly on the available sites, for example, in austenite different components mix on different sublattices. As instance, carbon mix on interstitial sublattices compared with, for example, nickel and chroumium which mix on substitutional sublattices. Therefore, in the case of a regular solution, for a two sublattice phase containing the components A, B, C and D where A, B mix on the first sublattice and C, D on the second, excess Gibbs free energy of mixing can be expressed as:

$$G_{mix}^{excess} = y_A^1 y_B^1 L_{A,B:*}^0 + y_C^2 y_D^2 L_{*:C,D}^0 \qquad [6]$$

where $L_{A,B:*}^0$ and $L_{*:C,D}^0$ are the regular solution parameters. The numbers 1,2 are the first and the second sublatice. y_i^j is the occupied site fraction. These parameters are independent from the nature of the occupied site on other sublattice. However, mutual interactions induced by the other occupied sublattice can be introduced as follows:

$$G_{mix}^{excess} = y_A^1 y_B^1 y_C^2 L_{A,B:C}^0 + y_A^1 y_B^1 y_D^2 L_{A,B:D}^0 + y_C^2 y_D^2 y_A^1 L_{A:C,D}^0 + y_C^2 y_D^2 y_B^1 L_{B:C,D}^0 \qquad [7]$$

Temperature dependency is considered through expressing the parameters as a polynomial functions of T and $\ln T$. The coefficients of the polynomials are stored in the SGTE (Scientific Group Thermodata Europe) databases on which MTDATA depends.

For a phase i, the free energy as an extensive thermodynamic property can be expressed as a function of temperature, pressure and composition as follows:

$$G_i = G_i(T, P, x_{i1}, x_{i2}, ..., x_{ij}) \qquad [8]$$

The free energy of the system can be written as:

$$G_{System} = \sum_{i}^{n} N_i G_i \qquad [9]$$

where G_i is the partial molar free energy of phase i. As such, since the calculation of the free energy is possible, predicting the equilibrium state is essentially mathematical.

Free energy calculation using MTDATA is based on selecting the appropriate database which obviously depends on the nature of the analysed systems.

User input

Free energy $\Delta G^{\alpha\gamma}$ was estimated (in J mol^{-1}) using the austenite chemical composition calculated for each alloy. A sample of the input (austenite chemical composition in wt%) is given below:

```
Fe,Cr,Co,Ni,Mo,Mn,Si,Al,Cu,V,Nb,W,C
1
95.186588
0
0
0
0
1.48317
1.97756
0.036585
0
0
0
0
1.3
```

with the leading “1” denotes that inputs are in wt%.

Output

A sample of the output is given underneath:

```
Using mpi file: T0_data.mpi
 Scanning temperature range:   273. --   1073.
 Precision for equal gibbs energy:   0.1
 Temp/K      Ferr.      Aust.
 908.00 -0.38068E+05 -0.39499E+05
 903.00 -0.37741E+05 -0.39160E+05
 898.00 -0.37416E+05 -0.38823E+05
 893.00 -0.37092E+05 -0.38486E+05
 888.00 -0.36769E+05 -0.38150E+05
 883.00 -0.36447E+05 -0.37815E+05
 878.00 -0.36127E+05 -0.37481E+05
 873.00 -0.35808E+05 -0.37148E+05
 868.00 -0.35490E+05 -0.36816E+05
 863.00 -0.35174E+05 -0.36484E+05
 858.00 -0.34858E+05 -0.36154E+05
 853.00 -0.34544E+05 -0.35824E+05
 848.00 -0.34232E+05 -0.35495E+05
 843.00 -0.33920E+05 -0.35167E+05
 838.00 -0.33610E+05 -0.34840E+05
 833.00 -0.33300E+05 -0.34514E+05
 828.00 -0.32993E+05 -0.34189E+05
 823.00 -0.32686E+05 -0.33865E+05
 818.00 -0.32380E+05 -0.33542E+05
```

“Ferr.” stands for ferrite and “Aust.” stands for austenite.

References

1) H. K. D. H. Bhadeshia: Materials Modelling, M.Phil. lecture notes (2003).

2) T. Sourmail: *Simultaneous Precipitation Reactions in Creep-Resistant Austenitic Stainless Steels*, Ph.D. thesis, University of Cambridge (2002).

3) H. Davis: MTDATA, National Physical Laboratory, Teddington, U.K. (2003).

4) K. Hack, editor: *The SGTE Casebook*, The IoM, London (1996).

Bibliography

1. O. Matsumura, Y. Sakura and H. Takechi: Scripta Metallurgica **21** (1987) 1301.
2. P. Jacques, A. Mertens, E. Girault, J. Ladrière and F. Delannay: Metall. and Mat. Trans., *submitted* (1999).
3. W. C. Jeong, D. K. Matlock and G. Krauss: Mater. Sci. Engng. **A165** (1993) 1.
4. K. Sugimoto, N. Usui, M. Kobayashi and S. Hashimoto: ISIJ Int. **32** (1992) 1311.
5. Y. Sakuma, D. K. Matlock and G. Krauss: Metall. and Mat. Trans. **23A** (1992) 1221.
6. V. F. Zackay, E. R. Parker, D. Fahr and R. Bush: Trans. Am. Soc. Met. **60** (1967) 252.
7. P. Haasen, editor: Materials Science and Technology, *Phase Transformations in Materials*, Volume **5**, Weinheim (Germany) (1991).
8. H. K. D. H. Bhadeshia: *Bainite in Steels*, 2nd edition, Institute of Materials, London (2001).
9. K. W. Andrews: J. Iron Steel Inst. **203** (1965) 721.
10. D. T. Llewellyn: Steels: *Metallurgy and Applications*, Oxford (1992).
11. O. Matsumura, Y. Sakuma and H. Takechi: Trans. ISIJ **27** (1987) 570.
12. J. Wang and S. van der Zwaag: Metall. and Mat. Trans. **32A** (2001) 1527.
13. P. Jacques, E. Girault, Ph. Harlet, and F. Delannay: ISIJ Int. **41** (2001) 1061.
14. D. A. Porter and K. E. Easterling: *Phase Transformations in Metals and Alloys*, 2nd edition, Chapman and Hall, London (1981).
15. A. Itami, M. Takahashi and K. Ushioda: ISIJ Int. **35** (1995) 1121.
16. K. Sugimoto, M. Misu, M. Kobayashi and H. Shirasawa: ISIJ Int. **33** (1993) 775.
17. W. C. Jeong and J. H. Chung: *HSLA Steels: Processing, Properties and Applications*, ed. By G. Tither and Z. Shoubua, Min., Met. And Mat. Soc., Warrendale, PA, (1992), 305.

18. H. K. D. H. Bhadeshia and D. V. Edmonds: Metall. and Mat. Trans. **10A** (1979) 895.
19. A. Pichler, P. Stiaszny, R. Potzinger, R. Tikal and E. Werner: Proc. 40th MWSP Conf., ISS, Warrendale, (1998), 259.
20. J. Chance and N. Ridley: Metall. and Mat. Trans. **12A** (1981) 1205.
21. B. P. J. Sandvik: Metall. and Mat. Trans. **13A** (1982) 789.
22. T. Nakamura and S. Nagakura: International Conference on Martensitic Transformations-ICOMAT-86, Japan Institute of Metals (1986) 386.
23. A. K. Taylor, G. B. Olson, M. Cohen and J. B. Vander Sande: Metall. and Mat. Trans. **20A** (1989) 2717.
24. A. K. Taylor, L. Chang, G. B. Olson, G. D. W. Smith, M. Cohen and J. B. Vander Sande: Metall. and Mat. Trans. **20A** (1989) 2749.
25. S. S. Babu, K. Hono and T. Sakuri: Applied Surface Science **67** (1993) 321.
26. M. De Meyer, D. Vanderschueren and B. C. De Cooman: ISIJ Int. **39** (1999) 813.
27. A. Perlade, O. Bouaziz and Q. Furnémont: Mater. Sci. Engng. A, *in press*.
28. I. Tamura: Metal Science **16** (1982) 245.
29. H. Y. Yu: Metall. and Mat. Trans. **28A** (1997) 2499.
30. J. R. Patel and M. Cohen: Acta Metallurgica **1** (1953) 531.
31. M. Cohen: International Summer Course on Martensitic Transformations. Leuven: Dep. Met. & Mat. Eng., KV Leuven, 1.1-1.12.
32. K. Sugimoto, M. Kobayashi and S. Hashimoto: Metall. and Mat. Trans. **23A** (1992) 3085.
33. G. B. Olson and M. Cohen: Metall. and Mat. Trans. **6A** (1975) 791.
34. T. Angel: J. Iron Steel Inst. **177** (1954) 165.
35. W. W. Gerberich, G. Thomas, E. R. Parker, and V. F. Zackay: Proc. Second Int. Conf. on 'Strength of metals and alloys', Vol. **3**, 894; 30 August-4 September 1970, Metals Park, Ohio, USA, ASM.
36. D. C. Ludwigson and J. A. Berger: J. Iron Steel Inst. **207** (1969) 63.
37. J. R. C. Guimarães: Scripta Metallurgica **6** (1972) 795.

38. F. Lecroisey and A. Pineau: Met. Trans. **3** (1972) 387.

39. P. L. Manganon and G. Thomas: Met. Trans. **1** (1970) 1577.

40. J. A. Venables: Phil. Mag. **7** (1964) 35.

41. H. Davis: *MTDATA*, National Physical Laboratory, Teddington, U.K. (2003).

42. Y. Tomita and K. Morioka: Materials Characterisation **38** (1997) 243.

43. P. Jacques, Q. Furnémont, A. Mertens and F. Delannay: Phil. Mag. A **81** (2001) 1789.

44. K.Sugimoto, M. Kobayashi, A. Nagasaka and S. Hashimoto: ISIJ Int. **35** (1995) 1407.

45. L. C. Chang and H. K. D. H. Bhadeshia: Mater. Sci. Engng. **A184** (1994) L17-L19.

46. I. Yu. Pyshmintsev, M. de Meyer, B. C. de Cooman, R. A. Savray, V. P. Shveykin and M. Vermeulen: Metall. and Mat. Trans. **33A** (2002) 1659.

47. M. Takahashi and H. K. D. H. Bhadeshia: Mater. Trans. JIM **32** (1991) 689.

48. S. B. Singh and H. K. D. H. Bhadeshia: Mater. Sci. Engng. **A245** (1998) 72.

49. W. C. Jeong, D. K. Matlock and G. Krauss: Mater. Sci. Engng. **A165** (1993) 9.